



**Production of High-Yield Short-Chain Oligomers or Glucose  
from Cellulose via Selective Hydrolysis in Molten Salt  
Hydrates and Separation**

Journal:	<i>Green Chemistry</i>
Manuscript ID	GC-ART-07-2019-002297.R1
Article Type:	Paper
Date Submitted by the Author:	07-Aug-2019
Complete List of Authors:	<p>Fan, Wei; University of Massachusetts, USA, Chemical Engineering  Liu, Qiyu; Department of Thermal Science and Energy Engineering  University of Science and Technology of China, Department of Thermal  Science and Energy Engineering  Ma, Qiaozhi; Laboratory of Basic Research in Biomass Conversion and  Utilization, University of Science and Technology of China  Sabnis, Sanket; University of Massachusetts, USA, Chemical Engineering  Zheng, Weiqing; University of Delaware, Department of Chemical and  Biomolecular Engineering  Vlachos, Dion; Univ. of Delaware,  Li, Wenzhi; Department of Thermal Science and Energy Engineering  University of Science and Technology of China, Department of Thermal  Science and Energy Engineering  Ma, Longlong; Guangzhou Institute of Energy Conversion, Chinese  Academic of Sciences, Key Laboratory of Renewable Energy</p>

## ARTICLE

# Production of High-Yield Short-Chain Oligomers from Cellulose via Selective Hydrolysis in Molten Salt Hydrates and Separation

Received 00th January 20xx,  
Accepted 00th January 20xx

DOI: 10.1039/x0xx00000x

Qiyu Liu,<sup>a,b</sup> Qiaozhi Ma,<sup>c</sup> Sanket Sabnis,<sup>b</sup> Weiqing Zheng<sup>d,e</sup>, Dionisios G. Vlachos<sup>d,e</sup>, Wei Fan,<sup>\*b,e</sup> Wenzhi Li,<sup>\*a</sup> and Longlong Ma<sup>\*a,f</sup>

Molten salt hydrates (MSH) are unique in overcoming the characteristic recalcitrance of crystalline cellulose. We show that cellulose can be efficiently hydrolyzed into short-chain oligomers and glucose under mild conditions in concentrated LiBr solution without using any additional acid catalyst. Under optimized reaction conditions, short-chain oligomers with a yield of 90.4% can be obtained. Selective hydrolysis in the MSH is effective even at a high initial cellulose concentration (higher than 10 wt.%). The obtained oligomers are solvated and soluble in the MSH. We show that amorphous carbon of a large surface area is effective for adsorption of the short-chain oligomers, cellobiose, and glucose from the MSH. The adsorption capacity and adsorption affinity of the carbon increases by ~4 and ~15 times in MSH with increasing the oligomer chain length compared to glucose and is negatively influenced by the ion concentration of the MSH. A stepwise hydrolysis process for converting crystalline cellulose into glucose is developed, whereby cellulose is firstly hydrolyzed into soluble short-chain oligomers in the MSH. The oligomers are then separated from the MSH using amorphous carbon and finally hydrolyzed into glucose under mild reaction conditions.

## Introduction

Lignocellulosic biomass is a promising renewable source for sustainable production of fuels and chemicals.<sup>1</sup> One of key challenges in biomass conversion is saccharification of cellulose into glucose.<sup>2-4</sup> The extensive intra- and inter-chain hydrogen bonds among cellulose limit access of both homogeneous and heterogeneous catalysts to  $\beta(1\rightarrow4)$  glycosidic linkages in the cellulose structure.<sup>5</sup> To address this challenge, several methods have been developed.<sup>6-8</sup> One promising method employs ionic liquids or molten salt hydrates (MSH) to dissolve crystalline cellulose, which can facilitate the cleavage of  $\beta(1\rightarrow4)$  glycosidic linkages in cellulose structures.<sup>5,9-11</sup> A proposed mechanism for the dissolution of cellulose in ionic liquids involves interactions between the anions of ionic liquid and the hydroxyls of cellulose

via hydrogen bonds.<sup>12, 13</sup> In MSH, cations interact with the oxygen of cellulose<sup>14</sup> and highly electronegative halogen ions act as hydrogen-bond acceptors of -OH groups of cellulose breaking its hydrogen bonds.<sup>15, 16</sup> In general, ionic liquids are expensive and require extensive organic synthesis, and certain ones are toxic.<sup>17, 18</sup> Additionally, the difficulty in recycling ionic liquids also limits their commercial application.<sup>19, 20</sup> MSHs, e.g., LiBr and ZnCl<sub>2</sub>, prepared with water to salt molar ratio equal or less than the coordination number of the cations, are effective in cellulose hydrolysis.<sup>5, 10, 21</sup> More than 90% glucose yield is obtained from cellulose hydrolysis in MSH at 85 °C especially when a small fraction of an inorganic acid is added.<sup>5, 22</sup> Compared to ionic liquids, MSH has a simple structure, is easy to synthesize and can be operated under a wide range of conditions. Despite its promising potential for cellulose hydrolysis, there are still several challenges in its use. One entails the economical separation of the produced sugar from the hydrolysate due to the high solubility of sugars in MSH.<sup>5, 23</sup> The primary solvation shell around the glucose ring consists predominantly of halogen anions which bind to the hydroxyl groups of glucose by hydrogen bonds, making separation of glucose difficult.<sup>24</sup> In order to address the separation issue, a biphasic reaction system is often used to convert glucose to 5-hydroxymethylfurfural (HMF) in MSH with parallel extraction of HMF to an organic phase.<sup>22</sup> However, direct separation of sugars from MSH without converting them into other chemicals is still highly desired because of their value and additional conversion pathways sugars provide.

<sup>a</sup> Department of Thermal Science and Energy Engineering, University of Science and Technology of China, Hefei, 233022, China.  
E-mail: liwenzhi@ustc.edu.cn

<sup>b</sup> Department of Chemical Engineering, University of Massachusetts-Amherst, 159 Goessman Lab, 686 N Pleasant Street, Amherst, 01003, USA.  
E-mail: wfan@engin.umass.edu

<sup>c</sup> College of Materials and Energy, South China Agricultural University, Guangzhou, 510642, China.

<sup>d</sup> Catalysis Center for Energy Innovation, University of Delaware, Newark, Delaware 19716; USA

<sup>e</sup> Department of Chemical and Biomolecular Engineering, University of Delaware, Newark, Delaware 19716

<sup>f</sup> Guangzhou Institute of Energy Conversion, Chinese Academy of Sciences, Guangzhou, Guangdong 510640, China.  
E-mail: mall@ms.giec.ac.cn

†Electronic Supplementary Information (ESI) available.

Amorphous carbon materials with functional surface groups have recently received significant attention as catalysts and adsorbents for the aqueous phase hydrolysis of cellulose to glucose due to their low cost, hydrothermal stability and unique adsorption properties.<sup>25-27</sup> Amorphous carbons with a high carbon content (>80%) are composed of polycyclic aromatic domains in irregular arrangements. Recently, Fukuoka et al. and Katz et al. have reported that the interaction between  $\beta(1\rightarrow4)$  glucan oligomers and highly carbonaceous amorphous carbon is dominated by the CH- $\pi$  hydrogen bonds.<sup>28, 29</sup> The adsorption of glucan oligomers on amorphous carbon from water, which is both enthalpically and entropically driven, increases with increasing chain length of the  $\beta(1\rightarrow4)$  glucan oligomer due to an increase in the interaction between the glucan and the carbon surface and the number of water molecules being released per anhydroglucose unit. Amorphous carbon, therefore, exhibits significantly improved adsorption capacity for glucan oligomer compared to glucose. However, due to the low solubility of glucan oligomers in water, use of amorphous carbon to separate the glucan oligomers from the aqueous hydrolysate of cellulose is hindered. Therefore, a well-known approach for hydrolyzing cellulose is to completely hydrolyze cellulose into glucose followed by separation of the produced glucose using different separation techniques, including using amorphous carbon-based adsorption methods.<sup>30, 31</sup> These processes though are fairly costly.

Interestingly, cellulose can be solvated in MSH by breaking hydrogen bonds, and further hydrolyzed into glucan oligomers under mild conditions. Glucan oligomers in MSH have the following features: (1) solvated and soluble in MSH and can be separated from the hydrolysate with adsorbents; (2) easy to be selectively converted into glucose under mild conditions. To address the challenge in selective hydrolysis of cellulose into glucose, we develop a stepwise hydrolysis process using MSH where cellulose is selectively hydrolyzed into short-chain glucan oligomer and the oligomers are separated from the MSH using amorphous carbon. The short-chain glucan oligomers can then be further hydrolyzed into glucose under mild conditions with a high selectivity.<sup>32, 33</sup> Our choice of separating glucan oligomers from MSH stems from not only being solvated and dissolved in MSH but importantly they can adsorb on carbon adsorbents with higher adsorption strength and capacity than glucose. The stepwise hydrolysis process opens a new approach to effectively hydrolyze cellulose and recover the sugars with low cost separation. This process also provides an alternative method to produce to short-chain oligomers, which have potential applications in polymer production, agriculture, and food science.<sup>34-36</sup> Compared with current saccharification technologies including enzymatic hydrolysis and acid hydrolysis, the process reported in this study utilizes no hazardous chemicals and is conducted at mild conditions. In addition, the separation method for short-chain oligomers provides an improved efficiency approach for the saccharification of cellulose which is a bottleneck for utilization of lignocellulose.

## Experimental section

### Materials

Glucose (99%), microcrystalline cellulose, lithium bromide (LiBr, 99%), 5-hydroxymethyl-2-furaldehyde (HMF, 97%), pyridine (anhydrous, 99.5+%) and phenyl isocyanate (98+%) were purchased from Alfa Aesar, Ltd., USA. Tetrahydrofuran (THF, 99.9%) and hydrogen peroxide (31.4%) were purchased from Fisher Scientific. Powered activated carbon Shirasagi M and Norit@ SX Ultra were purchased from Japan EnviroChemicals, Ltd., Japan and the black pearls 2000 (BP2000) was purchased from Cabot, Ltd. H-BEA zeolite with a Si/Al of 300 (CP811C-300) was purchased from Zeolyst International, Ltd.

### Hydrolysis in MSH and detection of oligomer

MSH was prepared by dissolving 18 g of LiBr in 12 g of deionized water, forming an MSH with 60 wt.% LiBr. Hydrolysis was carried out by mixing a specific amount of cellulose (0.5 g to 4 g) with 30 g of MSH in a 30 mL stainless Parr reactor at 130 °C for different reaction times with a stirring rate of 600 rpm. The reaction time varied from 1 h to 15 h. After the hydrolysis reaction, the reactor was cooled down to room temperature with circulating water.

Glucose and HMF were quantified by high performance liquid chromatography (HPLC) after 10 times dilution of the solutions. The HPLC (LC-20AT, Shimadzu) was equipped with refractive index (RID-10A) and UV-Vis (SPD-2AV) detectors. A Bio-Rad HPX-87H HPLC column with a guard column was used for product separation at an oven temperature of 85 °C. HPLC grade dilute sulfuric acid (0.1 mmol/L, Fisher) was used as a mobile phase with a flow rate of 0.6 mL/min.

After hydrolysis, the hydrolysate was filtered with a 0.22  $\mu\text{m}$  filter paper to separate the glucose, HMF and soluble oligomers from the insoluble part. After the filtration, the soluble products in the solution were analyzed. The glucose and HMF concentrations were measured by HPLC after 10 times dilution of the solution with water. The concentration of oligomer was measured by hydrolysis of the formed oligomers into glucose using a dilute acid following the method developed by the National Renewable Energy Laboratory (NREL). Namely, 1 g of hydrolysate obtained from the hydrolysis in MSH was mixed with 5 g of 4 wt.%  $\text{H}_2\text{SO}_4$  in a 15 mL thick wall glass reactor. Then the reactor was put into an oil bath at 130 °C for 1 h with magnetic stirring at 600 rpm. After the process, the reactor was taken out and cooled down to room temperature. The solution was analyzed using HPLC.

The product yields in hydrolysate are calculated using eqn (1-3):

$$\text{Glucose yield } (Y_G) = \frac{M_{GH}}{M_{GC}} \times 100\% \quad (1)$$

$$\text{HMF yield } (Y_H) = \frac{M_{HH}}{M_{GC}} \times 100\% \quad (2)$$

$$\text{Oligomers yield } (Y_G) = \left( \frac{M_{GOH}}{M_{GC}} - Y_G \right) \times 100\% \quad (3)$$

Here  $M_{GH}$  and  $M_{HH}$  are the moles of glucose and HMF in hydrolysate after MSH hydrolysis, respectively.  $M_{GOH}$  are the moles of glucose in dilute acid hydrolysate after oligomers hydrolysis and  $M_{GC}$  are the moles of glucose units in raw cellulose.

### Molecular weight measurement of oligomers

The molecular weight of the products in the hydrolysate was analyzed by gel permeation chromatography (GPC) and Matrix Assisted Laser Desorption Ionization (MALDI, Bruker Instruments, Billerica MA). Before the measurement, a two-step pretreatment process was carried out. Dialysis was used to remove LiBr from the hydrolysates. 5 g of hydrolysates obtained from the hydrolysis in MSH was added into 15 cm of a dialysis tube (T3, Cellu-Sep) without further purification. The tube was sealed with two plastic grips. Dialysis was performed in a 1000 mL glass breaker filled with deionized water under a magnetic stirring of 100 rpm. The dialysis was repeated two times. After the dialysis process, the solution inside the tube changed from a yellow transparent solution to a white flocculent precipitate (Fig. S2 in the ESI.†). The precipitate was removed from the dialysis tube and further dried in a rotary evaporator at 60 °C.

The solid samples were functionalized before the GPC and MALDI measurements using a method reported in literature.<sup>37, 38</sup> Cellulose and the products obtained from the hydrolysis of raw cellulose in the MSH at 130 °C for 1 h, 3 h and 5 h, were analyzed. The dried solid sample (5 mg) obtained from dialysis and phenyl isocyanate (0.2 mL) were added into a 15 mL thick-wall glass tube (Synthware, Beijing) together with 2 mL of anhydrous pyridine. After stirring at 80 °C for 24 h, the mixture became a yellow transparent solution. 0.5 mL of methanol was then added to terminate the reaction between the solid sample and phenyl isocyanate. Finally, the solvent was removed in a vacuum oven at 65 °C overnight. The product was dissolved in tetrahydrofuran (THF), and analyzed by GPC and MALDI.

For GPC measurements, samples were dissolved in THF, the column and RI detector were kept at 40 °C and flow rate was set at 1 mL/min with THF as a mobile phase. Agilent 1260 with three 7.5 × 300 mm PL-gel mix C columns with a particle size of 5 μm was used in the GPC measurement. The molecular weight was measured against polymethyl methacrylate (PMMA) standards with molecular weight ranging from 60,000 to 300,000.

For MALDI measurements, samples were dissolved in THF, and mixed 1:1 with a 10 mg/mL solution of 2,5-dihydroxybenzoic acid. The solution was vortexed briefly and then 1 μL was spotted on a stainless steel MALDI target. Data were acquired in positive ion linear mode using minimum laser fluency to obtain adequate signal. Data was collected over a range 1000 m/z - 12000 m/z.

### Adsorption of glucose, cellobiose, and oligomers

Activated carbon and H-BEA zeolite were dried at 100 °C for 24 h before employed in adsorption. Due to poor dispersion of BP2000 carbon black in the MSH, the carbon was treated with H<sub>2</sub>O<sub>2</sub> to introduce oxygen-containing groups on the surface. 1 g of BP2000 was added into a 50 mL centrifuge tube with 20 g of 31.4 wt.% H<sub>2</sub>O<sub>2</sub>. The mixture was stirred at room temperature for 12 h. The obtained

sample named OX-BP2000 was then washed with deionized water until the pH of the supernatant was neutral. BP2000 and OX-BP2000 were characterized by an X-ray photoelectron spectrometer (Thermo-Fisher, equipped with a monochromatic Al Kα X-ray source with 400 μm analysis spot size).

For glucose and cellobiose adsorption, glucose or cellobiose solutions were prepared with LiBr concentration of 0 wt.%, 10 wt.%, 30 wt.% and 60 wt.%. The initial substrate concentration was varied from 1.6 mg/mL to 30.0 mg/mL. For adsorption, 40 mg of the adsorbent was added into a 5 mL glass vial (Fisher Scientific) together with 3 g of saccharide solution, and stirred at 800 rpm for 24 h. After adsorption, the liquid phase was separated from the solid adsorbent by centrifugation at 6000 rpm. The liquid was diluted 10 times using deionized water before HPLC measurement. The adsorption capacity was calculated using following eqn (4-5):

$$\text{Glucose adsorbed } (Y_{\text{carbon}}) = \frac{(M_{GI} - M_{GF})}{M_A} \times 100\% \quad (4)$$

$$\text{Cellobiose adsorbed } (Y_{\text{carbon}}) = \frac{(M_{CI} - M_{CF})}{M_A} \times 100\% \quad (5)$$

where  $M_A$  is the amount of the adsorbent;  $M_{GI}$  and  $M_{CI}$  are the initial glucose and cellobiose amount in solution before the adsorption, respectively;  $M_{GF}$  and  $M_{CF}$  are the equilibrium glucose and cellobiose amount in solution after the adsorption, respectively.

For oligomer adsorption, the hydrolysate obtained from the hydrolysis in MSH (0.5 g of cellulose, 30 g of MSH, 130 °C, 5 h) was diluted with LiBr solution, resulting in a series of solutions with different oligomer concentrations from 0.3 mg/mL to 4.0 mg/mL and LiBr concentration from 10 wt.% to 60 wt.%. The absence of data at 0 wt.% LiBr solution is because the oligomers are insoluble in water (Fig. S2). 40 mg of adsorbent was mixed with 3 g of prepared solution in a 5 mL glass tube. After stirring for 12 h, the liquid was separated from the adsorbent by centrifugation at 6000 rpm for 10 min.

The concentration of oligomer in the liquid was measured by the hydrolysis of the formed oligomers into glucose using the method described earlier. The oligomers adsorption capacity was calculated using the following eqn. (6):

$$\text{Oligomer adsorbed } (Y_{\text{carbon}}) = \frac{(M_{OI} - M_{OF})}{M_A} \times 100\% \quad (6)$$

where  $M_A$  is the amount of the adsorbent;  $M_{OI}$  is the initial oligomer amount in solution before the adsorption;  $M_{OF}$  is the equilibrium oligomer amount in solution after the adsorption.

## Results and discussion

Acidified LiBr molten salt hydrate (MSH) is an efficient solvent for crystalline cellulose exfoliation and conversion into glucose.<sup>5</sup> In order to selectively produce oligomers rather than glucose in the MSH, crystalline cellulose was mixed with 60 wt.% LiBr solution without adding any acid catalyst. It was observed that the product distribution varied with reaction time and initial cellulose concentration. As shown in Fig. 1a, a negligible amount of soluble oligomers were detected after 1 h and 3 h of

treatment in the MSH, suggesting that cellulose depolymerisation was insufficient, and products in the hydrolysates were insoluble in the MSH and filtered out from the MSH before the measurement. Oligomer yield rapidly increased to 90.4% with a small amount of detectable glucose and HMF after reacting for 5 h, indicating cellulose hydrolysis can be selectively controlled to produce a high yield of oligomer. The obtained oligomer seems to be soluble in the MSH since no precipitation was observed and the hydrolysate can go through the 0.22  $\mu\text{m}$  filter paper without reducing the oligomer concentration in the filtrate (Fig. S3 and Fig. S4 in the ESI.†). After removing LiBr from the hydrolysates by dialysis, white solid precipitation was observed, suggesting that the oligomers are insoluble in water. This result is consistent with the previous literature indicating that the solubility of cellulose and oligomers can be largely enhanced in MSH.<sup>39</sup> Due to the lower molecular weight and less rigid structure of the oligomers, compared to crystalline cellulose, the oligomers can be selectively converted into glucose with dilute homogeneous acid catalyst in water with high yield.<sup>33, 40</sup> This observation motivated the development of a stepwise process to hydrolyze cellulose into short-chain glucan oligomers in the MSH, separate the oligomers from the MSH and further hydrolyze the oligomers into glucose. Further increasing reaction time led to the formation of glucose and HMF. The glucose yield increased with time from 5 h to 11 h followed by a slight decrease at 15 h. The highest glucose yield was 75.3% at 11 h, suggesting that cellulose can be selectively hydrolyzed to glucose in the MSH without using additional acid catalyst. The slight decrease of glucose yield from 11 h to 15 h is due to the further dehydration of glucose to HMF and possible formation of humins. The highest glucose yield is comparable to the published work using imidazolium-based ionic liquids and acid catalyst. For example, Blake and Seema used hydrochloric acid and ionic liquid  $[\text{C}_4\text{mim}]\text{Cl}$  to hydrolyze switchgrass, and a maximum yield of 53% glucose and 88% xylose were recovered.<sup>41</sup> A scale-up

acidolysis of municipal solid waste/corn stover blends in  $[\text{C}_4\text{C}_1\text{Im}]\text{Cl}$  showed 58% glucose and 87% xylose yield.<sup>42</sup>

The effect of initial cellulose concentration on the oligomer yield was also studied. The product distributions after treating cellulose in the MSH at 130  $^\circ\text{C}$  for 5 h are shown in Fig. 1b. It was found that the oligomer yield decreased with an increase in cellulose concentration, namely from 90.4% to 47.7% when the cellulose amount ranged from 0.5 g to 3 g in 30 g of MSH. The product distributions remained nearly constant with increasing the amount of cellulose from 3 g to 4 g. The carbon balance also decreased from 94.8% to 79.8% with increase in cellulose amount from 0.5 g to 4 g. These results suggest that the MSH can hydrolyze cellulose into oligomers and glucose over a wide range of concentrations, which is desirable for practical applications. The highest solid-liquid weight ratio studied here is higher than 1:10, which is higher than the most other experiments using ionic liquids,<sup>3, 5</sup> underscoring the potential of LiBr MSH media. The overall carbon balance decreased with increasing the cellulose concentration which might be due to the higher yield of humins.

For the most concentrated cellulose solution (4 g of cellulose in 30 g of MSH), the effect of reaction time was also investigated (Fig. 1c). It was found that increasing the reaction time from 1 h to 3 h significantly changed the product distribution. Specifically, the oligomer yield sharply increased from 15.5% to 62.0%, indicating a faster depolymerization process compared to the case with 0.5 g of cellulose in 30 g of MSH (Fig. 1a). The oligomer yield decreased from 62.0% to 26.2% while the glucose yield increased from 12.3% to 47.2% upon increasing the reaction time further from 3 h to 6 h, suggesting further hydrolysis of oligomers to glucose. The overall carbon balance with a high initial concentration of cellulose was higher than 75%, demonstrating that the MSH can potentially be used over a wide range of cellulose concentrations under optimized reaction conditions.

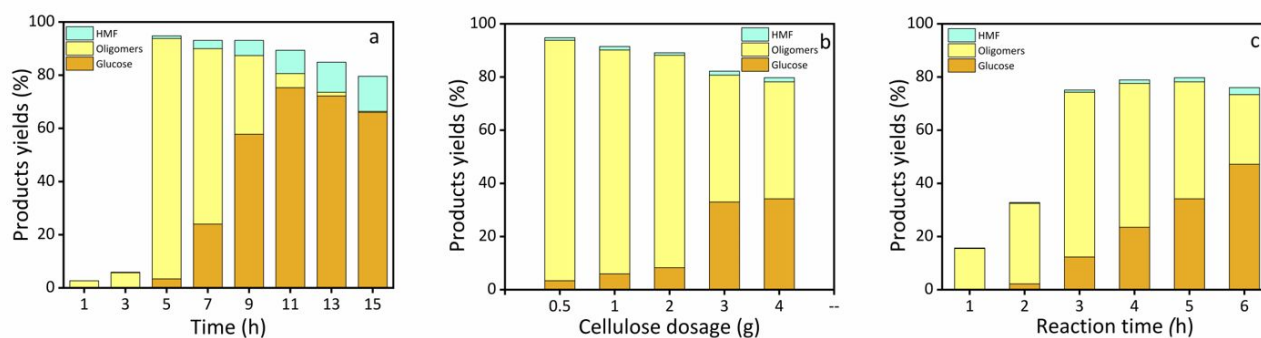


**Fig. 1.** (a) Product yields of glucose, HMF and oligomers for hydrolysis of cellulose in the LiBr MSH with 0.5 g of cellulose at different reaction times. Reaction conditions: 30 g of MSH, 130  $^\circ\text{C}$ ; (b) Product yields of glucose, HMF and oligomers for the hydrolysis of cellulose in the MSH with different initial cellulose concentrations. Reaction conditions: 30 g of MSH, 130  $^\circ\text{C}$  and 5 h; (c) Product yields of glucose, HMF and oligomers for the hydrolysis of cellulose in the MSH with 4 g of cellulose at different reaction times. Reaction conditions: 30 g of MSH and 130  $^\circ\text{C}$ .

The structure of the crystalline cellulose and products obtained after 1 h and 3 h of hydrolysis at 130  $^\circ\text{C}$  with a cellulose concentration of 0.5 g in 30 g of MSH were analyzed by GPC.

The average molar mass ( $M_w$ ) and degree of polymerization (DP) of those samples are listed in Table 1.

Table 1 The GPC analysis results of different samples<sup>a</sup>.

Samples	M <sub>w</sub>	DP <sup>b</sup>
Raw cellulose	211.1 K	406
Cellulose hydrolyzed for 1 h	135.3 K	260

<sup>a</sup>Mixture, M<sub>w</sub> and DP are average values. <sup>b</sup>The detailed DP calculation method is listed in the ESI.†

Weight-average molecular weight suggests that the DP of cellulose changed from 406 to 260 after 1 h of hydrolysis. Detection of the molecular weight of the products after 3 h of hydrolysis using the GPC method was not feasible due to the product low molecular weight. MALDI was also employed after 1 h, 3 h and 5 h of hydrolysis. Consistent with the GPC measurements, no product was detected after 1 h and 3 h of hydrolysis indicating that the molecular weight of the two samples is higher than 12,000. The sample after 5 h of hydrolysis exhibited oligomers with a DP ranging from 4 to 11 glucose units (Fig. 2). The DP of cellulose sharply decreased from 260 to less than 11 when the hydrolysis time increased from 1 h to 5 h, suggesting that the hydrolysis in the MSH can selectively be controlled to produce short-chain glucan oligomers. It should be noted that since neither the GPC nor the MALDI can detect products after 3 h, the DP of those products should be between 23 and 115 (the maximum detectable DP measured by MALDI is 23, and the minimum measurable DP by GPC is 115).

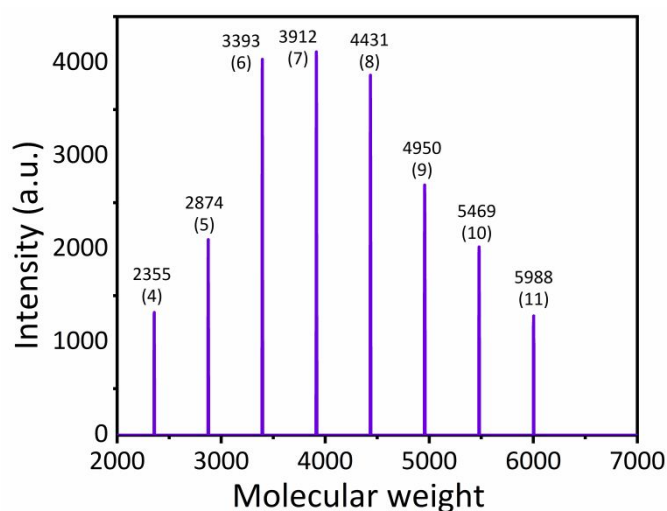


Fig. 2. Molecular weight distribution and DP (numbers in parenthesis) of 0.5 g cellulose hydrolysis in 30 g of LiBr MSH for 5 h at 130 °C.

Activated carbon, zeolite and OX-BP2000 were employed to adsorb the short-chain oligomers from the hydrolysates of cellulose in the MSH. Activated carbon is a well-known commercial adsorbent.<sup>43</sup> Zeolites are also effective for glucose adsorption.<sup>23</sup> Additionally, BP2000 has been used due to its high surface area and microporosity.<sup>40, 44, 45</sup> In order to improve the dispersion of BP2000 in the MSH, the surface of BP2000 was slightly oxidized using H<sub>2</sub>O<sub>2</sub>. The XPS results of BP2000 and BP2000 after oxidation (OX-BP2000) are shown in Fig. S5 and the elemental distribution of materials is shown in Table S2 in the ESI.†

The results in Fig. S5 and Table S2 indicate that hydrogen peroxide can increase the oxygenated functionalities on the surface of the carbon. The increased peaks at 285.6 eV and 286.5 eV are assigned to C-O bonds<sup>46</sup> while the 288.6 eV peak is attributed to the C=O species.<sup>46, 47</sup> The elemental distribution indicates a small increase in the oxygen percentage of the material after oxidation, which could enhance its hydrophilicity and dispersion in the MSH. More importantly, there is no obvious change of the peak shape at other abscissas in the XPS spectra, indicating that hydrogen peroxide causes limited change in the carbon structure.

The surface areas of OX-BP2000, activated carbon Shirasagi M, activated carbon Norit@ SX Ultra Cat and H-BEA zeolite were calculated from their nitrogen adsorption/desorption isotherms. The results are shown in Table 2. The surface area of OX-BP2000 is 1,437 g/m<sup>2</sup> which is the highest of all used adsorbents. The activated carbon Shirasagi M and Norit@ SX Ultra Cat have surface areas of 1,140 and 1,300 g/m<sup>2</sup>, respectively. H-BEA zeolite has the lowest surface area of 620 g/m<sup>2</sup>. The adsorption capacity of the adsorbents for the short-chain oligomers was measured by adding 40 mg of adsorbent into the MSH with a short-chain oligomer concentration of 26 mg/mL produced from 0.5 g of cellulose hydrolyzed in 30 g of the MSH for 5 h. Adsorption capacities of the short-chain oligomers on the adsorbents are shown in Table 2. The two activated carbons exhibited a slightly lower adsorption capacity than OX-BP2000. The result indicates that the adsorption capacity of the adsorbents might be related to surface area, but also can be affected by the presence of microporosity in OX-BP2000 and the oxygen containing groups on the surface. The adsorption of oligomer on H-BEA is lower than other three carbon adsorbents. However, taking the relatively lower surface area into consideration, H-BEA zeolite presents a high adsorption capacity per surface area at 0.13 mg/m<sup>2</sup>. This suggests that the zeolite is also effective in the oligomer adsorption. On account of the high adsorption capacity, OX-BP2000 was employed for further study. Additionally, the result of activated carbon Shirasagi M adsorption is also discussed in the ESI.†

Table 2 Surface areas and oligomers adsorption capacities on different adsorbents.

Material	Surface area (m <sup>2</sup> /g)	Adsorption capacity (mg/g)	Adsorption capacity per surface area (mg/m <sup>2</sup> )
OX-BP2000	1437	300	0.21
Shirasagi M	1140	205	0.18
Norit SX Ultra Cat	1300	260	0.20
H-BEA zeolite	620	80	0.13

<sup>a</sup> Adsorption capacity of different adsorbents toward oligomers. Oligomers preparation: 0.5 g cellulose in 30 g MSH, 130 °C, 5 h. Adsorption process: 40 mg adsorbent, 3 g hydrolysate, room temperature for 12 h.

Glucose, cellobiose and oligomers adsorption isotherms at different LiBr concentrations were measured on OX-BP2000 to further investigate the adsorption process. The adsorption isotherms of glucose and cellobiose at 0, 10, 30 and 60 wt.% LiBr concentration and short-chain oligomers at 10, 30 and 60 wt.%



LiBr concentration on OX-BP2000 were collected at room temperature. Three adsorption isotherms including Langmuir, Redlich-Peterson and Freundlich models were employed to fit the data. The fitting equations and results are shown in the ESI. † (adsorption isotherms in Fig. S6, Fig. S8 and Fig. S10, fitting parameters in Table S3, Table S4 and Table S5, respectively). Since the Redlich-Peterson isotherm gives the highest  $R^2$  value, it was chosen to fit and obtain the adsorption parameters from the glucose, cellobiose and short-chain oligomer adsorption isotherms on OX-BP2000 (Fig. 3), and the estimated parameters are shown in Table 3. The results clearly demonstrate that the increase of LiBr concentration has a negative effect on adsorption capacity, which might be due to adsorption of ions on adsorption sites of the adsorbents, reducing the adsorption

capacity. Comparing the adsorption capacities of glucose, cellobiose and short-chain oligomer on OX-BP2000, OX-BP2000 exhibits higher adsorption capacities for the oligomers of longer chain lengths. For example, the maximum adsorption capacities of glucose, cellobiose and short-chain oligomer in 10 wt.% LiBr are about 113, 300 and 350 mg/mL, while lower adsorption capacities of 72, 80 and 295 mg/mL were achieved in 60 wt.% LiBr, respectively. The preferred adsorption of short-chain oligomers compared to glucose and cellobiose could be due to (a) the short-chain oligomers adsorbed on carbon surface possessing a denser packing structure compared with cellobiose and glucose or (b) a part of the short-chain oligomer “dangles” off the carbon surface which leads to a high density of adsorbed oligomers.<sup>48</sup>

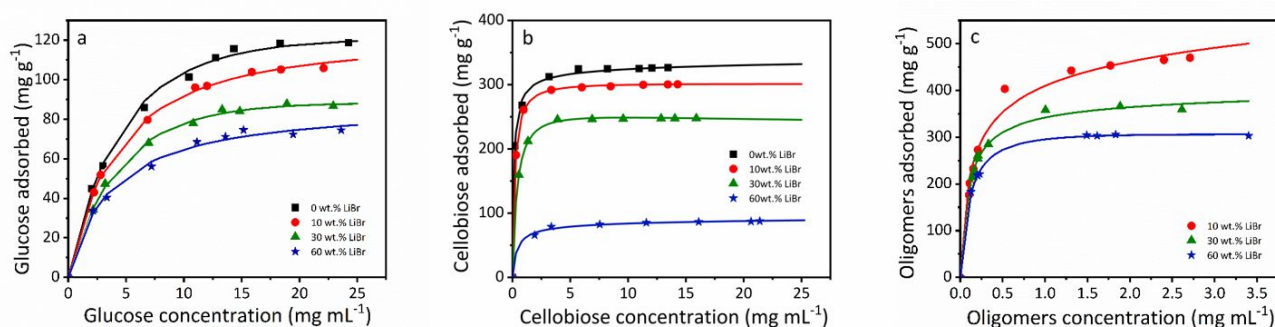


**Fig. 3.** Adsorption isotherms of (a) glucose, (b) cellobiose, and (c) oligomers on OX-BP2000 from LiBr MSH with concentration of 0, 10, 30 and 60 wt.% at room temperature (about 20 °C). The products concentrations are equilibrium concentrations after adsorption. Oligomers preparation: 0.5 g cellulose, 30 g MSH, 130 °C, 5 h. The points are from experimental measurements. The lines are from the Redlich-Peterson equation fitting.

**Table 3.** Redlich-Peterson fitting parameters for the adsorption of glucose, cellobiose and oligomer on OX-BP2000 at room temperature (20 °C).

Adsorbate	LiBr Solution	$K_{RP}$ (mL/g)	$b_{RP}$	$n_{RP}$	$R^2$
Glucose	0 wt.%	26.474	0.115	1.137	0.994
Glucose	10 wt.%	25.937	0.137	1.164	0.997
Glucose	30 wt.%	20.624	0.110	1.176	0.995
Glucose	60 wt.%	20.358	0.171	1.091	0.983
Cellobiose	0 wt.%	2837.214	9.033	0.981	0.988
Cellobiose	10 wt.%	1577.198	5.060	1.009	0.999
Cellobiose	30 wt.%	634.968	2.230	1.041	0.996
Cellobiose	60 wt.%	253.358	3.219	0.957	0.937
Oligomer	10 wt.%	5188.234	11.656	0.881	0.968
Oligomer	30 wt.%	4321.987	11.630	0.966	0.965
Oligomer	60 wt.%	3268.656	8.761	1.034	0.994

It was found that the glucose adsorption isotherms reach to their maximum adsorption capacity at an equilibrium glucose concentration (around 20 mg/mL), much higher than that of cellobiose (around 5 mg/mL) and oligomers (around 1 mg/mL), indicating that cellobiose and oligomer present a high adsorption affinity to OX-BP2000 with increased chain length. In order to further investigate the effect of chain-length as well as of the LiBr concentration on the adsorption affinity, Henry

constants were calculated. The  $K_{RP}$  values of Redlich-Peterson equation can be taken as the Henry constants in the limit of a dilute adsorbate solution<sup>48</sup> and the adsorption results in dilute (10 wt.%) and concentrated (60 wt.%) LiBr solutions are shown in Fig. 4. Fig. 4a shows that in 10 wt.% LiBr solution, the  $K_{RP}$  values increase from 25.94 mL/g to 1577.20 mL/g to 5188.23 mL/g with increasing the chain-length from glucose to cellobiose to oligomer. A similar trend was observed for the

adsorption in 60 wt.% LiBr solution, as shown in Fig. 4b. The result suggests that the adsorption affinity for the short-chain glucan oligomers on the carbon increases with the chain length and is around 15 times higher than that for glucose in the 60wt.% LiBr MSH. The results in Fig. 4a and Fig. 4b indicate that the increase of LiBr concentration has a negative effect on adsorption affinity in all cases. Specifically, upon increasing the LiBr concentration from 10 wt.% to 60 wt.%, glucose adsorption affinity decreases from 25.94 mL/g to 20.36 mL/g, cellobiose

adsorption affinity decreases from 1,577.20 mL/g to 253.36 mL/g, and oligomer adsorption affinity decreases from 5,188.23 mL/g to 3,268.66 mL/g. The adsorption equilibrium constants are lower than the adsorption of glucose and cellobiose on carbons from aqueous phase without any LiBr, further indicating the negative effect of LiBr on adsorption.

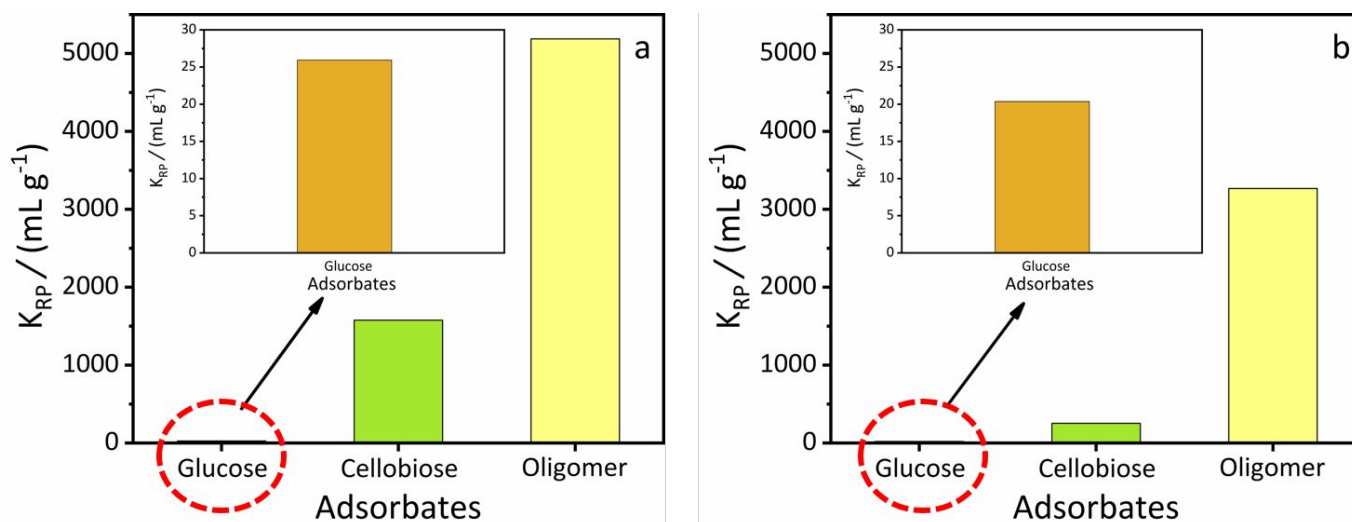
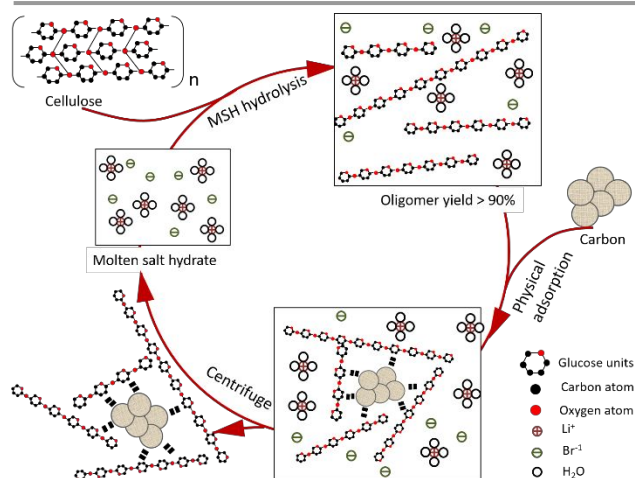


**Fig. 4.**  $K_{RP}$  values of glucose, cellobiose and oligomer on OX-BP2000 in (a) 10 wt.% LiBr solution and 60 wt.% LiBr solution. The parameters are from the Redlich-Peterson equation fitting.



**Scheme 1** Stepwise process of cellulose being hydrolyzed into oligomers in MSH followed by product separation.

## Conclusions

In summary, a stepwise method was introduced to selectively produce glucose from cellulose, as shown in Scheme 1. Cellulose was converted into short-chain glucan oligomers with a yield of more than 90% in LiBr MSH without any inorganic acid. The short-chain oligomers, consisting of 4-11 glucose units, are solvated and soluble in the MSH and can be effectively adsorbed and separated from the MSH through physical adsorption on

various materials, most notably amorphous carbon black. Importantly, we leverage the higher adsorption capacity and affinity of the amorphous carbon for glucan oligomers (by 4 and 15 times, respectively), compared to glucose in MSH to improve the separation. The obtained short-chain oligomers can be converted into glucose with a high selectivity using dilute homogeneous acid catalysts or used in other emerging applications in agriculture and healthcare.<sup>34, 49, 50</sup>

## Conflicts of interest

There are no conflicts to declare.

## Acknowledgements

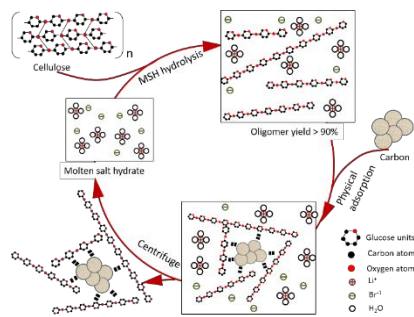
This project was supported by the Catalysis Center for Energy Innovation, an Energy Frontier Research Center funded by the US Dept. of Energy, Office of Science, and Office of Basic Energy Sciences under award number DE-SC0001004. The visit of Qiyu Liu to UMass Amherst was supported by a fellowship from the National Key R&D Program of China (2017YFE0106600) and Chinese Scholarship Council. The mass spectral data were obtained at the University of Massachusetts Mass Spectrometry Center.

## Notes and references



‡ Footnotes relating to the main text should appear here. These might include comments relevant to but not central to the matter under discussion, limited experimental and spectral data, and crystallographic data.

- §  
§§  
etc.
1. J. N. Chheda, G. W. Huber and J. A. Dumesic, *Angew. Chem. Int. Edit.*, 2007, **46**, 7164-7183.
  2. M. Mascal and E. B. Nikitin, *Angew. Chem. Int. Edit.*, 2008, **47**, 7924-7926.
  3. R. Rinaldi, R. Palkovits and F. Schüth, *Angew. Chem. Int. Edit.*, 2008, **47**, 8047-8050.
  4. W. Li, Q. Liu, Q. Ma, T. Zhang, L. Ma, H. Jameel and H.-m. Chang, *Bioresource Technol.*, 2016, **219**, 753-756.
  5. W. Deng, J. R. Kennedy, G. Tsilomelekis, W. Zheng and V. Nikolakis, *Ind. Eng. Chem. Res.*, 2015, **54**, 5226-5236.
  6. R. Rinaldi and F. Schüth, *ChemSusChem*, 2009, **2**, 1096-1107.
  7. I. P. Samayam, B. L. Hanson, P. Langan and C. A. Schall, *Biomacromolecules*, 2011, **12**, 3091-3098.
  8. K. Rajendran, E. Driellak, V. S. Varma, S. Muthusamy and G. Kumar, *Biomass Convers. and Bior.*, 2018, **8**, 471-483.
  9. C. Li and Z. K. Zhao, *Adv. Synth. & Catal.*, 2007, **349**, 1847-1850.
  10. S. Sen, J. D. Martin and D. S. Argyropoulos, *ACS Sustain. Chem. Eng.*, 2013, **1**, 858-870.
  11. A. Schenzel, A. Hufendiek, C. Barner-Kowollik and M. A. Meier, *Green Chem.*, 2014, **16**, 3266-3271.
  12. H. Wang, G. Gurau and R. D. Rogers, *Chem. Soc. Rev.*, 2012, **41**, 1519-1537.
  13. J. C. Duchemin, *University of Canterbury Mechanical Engineering*, 2008.
  14. E. Brendler, S. Fischer and H. Leipner, *Cellulose*, 2001, **8**, 283-288.
  15. B. Medronho and B. Lindman, *Curr. Opin. Colloid In.*, 2014, **19**, 32-40.
  16. Z. Jiang, J. Fan, V. L. Budarin, D. J. Macquarrie, Y. Gao, T. Li, C. Hu and J. H. Clark, *Sustain. Energ. Fuels*, 2018, **2**, 936-940.
  17. T. C. Brennan, S. Datta, H. W. Blanch, B. A. Simmons and B. M. Holmes, *BioEnergy Res.*, 2010, **3**, 123-133.
  18. T. P. T. Pham, C.-W. Cho and Y.-S. Yun, *Water Res.*, 2010, **44**, 352-372.
  19. C. Garkoti, J. Shabir and S. Mozumdar, *New J. Chem.*, 2017, **41**, 9291-9298.
  20. T. Vander Hoogerstraete, S. Wellens, K. Verachtert and K. Binnemans, *Green Chem.*, 2013, **15**, 919-927.
  21. X.-N. Lv, G. Li, F. Yang, P. Gao, Z.-h. Liu, L. Meng and X.-Q. Yu, *Ind. Eng. Chem. Res.*, 2012, **52**, 297-302.
  22. S. Sadula, O. Oesterling, A. Nardone, B. Dinkelacker and B. Saha, *Green Chem.*, 2017, **19**, 3888-3898.
  23. J. van den Bergh, W. Wiedenhof, D. Siwy and H. Heinerman, *Adsorption*, 2017, **23**, 563-568.
  24. T. Youngs, C. Hardacre and J. Holbrey, *J. Phys. Chem. B*, 2007, **111**, 13765-13774.
  25. S. Sugauma, K. Nakajima, M. Kitano, D. Yamaguchi, H. Kato, S. Hayashi and M. Hara, *J. AM Chem. Soc.*, 2008, **130**, 12787-12793.
  26. M. Kitano, D. Yamaguchi, S. Sugauma, K. Nakajima, H. Kato, S. Hayashi and M. Hara, *Langmuir*, 2009, **25**, 5068-5075.
  27. H. Kobayashi, M. Yabushita, T. Komanoya, K. Hara, I. Fujita and A. Fukuoka, *ACS Catalysis*, 2013, **3**, 581-587.
  28. A. Charmot, P.-W. Chung and A. Katz, *ACS Sustainable Chemistry & Engineering*, 2014, **2**, 2866-2872.
  29. M. Yabushita, H. Kobayashi, J. y. Hasegawa, K. Hara and A. Fukuoka, *ChemSusChem*, 2014, **7**, 1443-1450.
  30. K. Kuroda, K. Miyamura, H. Satria, K. Takada and K. Takahashi, *ACS Sustain. Chem. Eng.*, 2016, **4**, 3352-3356.
  31. P. Dornath, S. Ruzycky, S. Pang, L. He, P. Dauenhauer and W. Fan, *Green Chem.*, 2016, **18**, 6637-6647.
  32. Q. A. Nguyen, M. P. Tucker, F. A. Keller, D. A. Beaty, K. M. Connors and F. P. Eddy, *Twentieth Symposium on Biotechnology for Fuels and Chemicals*, 1999, 77-79, 133-142.
  33. A. Sluiter, B. Hames, R. Ruiz, C. Scarlata, J. Sluiter, D. Templeton and D. Crocker, *Laboratory Analytical Procedure*, 2008, **1617**, 1-16.
  34. P. Chen, A. Shrotri and A. Fukuoka, *ChemSusChem*, 2019, **12**, 1-6.
  35. C. A. Souza, S. Li, A. Z. Lin, F. Boutrot, G. Grossmann, C. Zipfel and S. C. Somerville, *Plant Physiol.*, 2017, **173**, 2383-2398.
  36. E. Billes, V. Coma, F. Peruch and S. Grelier, *Polym. Int.*, 2017, **66**, 1227-1236.
  37. B. B. Hallac, P. Sannigrahi, Y. Pu, M. Ray, R. J. Murphy and A. J. Ragauskas, *J. Agr. Food Chem.*, 2009, **57**, 1275-1281.
  38. S. Matsuoka, H. Kawamoto and S. Saka, *J. Anal. Appl. Pyrol.*, 2014, **106**, 138-146.
  39. S. Fischer, H. Leipner, K. Thümmel, E. Brendler and J. Peters, *Cellulose*, 2003, **10**, 227-236.
  40. P. Dornath and W. Fan, *Micropor. Mesopor. Mat.*, 2014, **191**, 10-17.
  41. N. Sun, H. Liu, N. Sathitsuksanoh, V. Stavila and B. M. Holmes, *Biotechnol Biofuels*, 2013, **6**, 39-39.
  42. C. Li, L. Liang, N. Sun, V. S. Thompson, F. Xu, A. Narani, Q. He, D. Tanjore, T. R. Pray and B. A. Simmons, *Biotechnol Biofuels*, 2017, **10**, 13.
  43. R. C. Bansal and M. Goyal, *Activated carbon adsorption*, CRC press, 2005.
  44. M. Kruk, M. Jaroniec and Y. Berezniński, *J. Colloid Interf Sci.*, 1996, **182**, 282-288.
  45. N. Rajabbeigi, R. Ranjan and M. Tsapatsis, *Micropor. Mesopor. Mat.*, 2012, **158**, 253-256.
  46. M. Chevalier, F. Robert, N. Amusant, M. Traisnel, C. Roos and M. Lebrini, *Electrochim. Acta*, 2014, **131**, 96-105.
  47. C. Hontoria-Lucas, A. López-Peinado, J. d. D. López-González, M. Rojas-Cervantes and R. Martín-Aranda, *Carbon*, 1995, **33**, 1585-1592.
  48. P. Dornath, S. Ruzycky, S. Pang, L. He, P. Dauenhauer and W. Fan, *Green Chem.*, 2016, **18**, 6637-6647.
  49. B. K. Knapp, L. L. Bauer, K. S. Swanson, K. A. Tappenden, G. C. Fahey and M. R. C. de Godoy, *Nutrients*, 2013, **5**, 396-410.
  50. T. Hasunuma, K. Kawashima, H. Nakayama, T. Murakami, H. Kanagawa, T. Ishii, K. Akiyama, K. Yasuda, F. Terada and S. Kushibiki, *Anim. Sci. J.*, 2011, **82**, 543-548.



Stepwise process of cellulose being hydrolyzed into oligomers in MSH followed by product separation.